

Density-Based Control of Air Coolers in Supercritical CO₂ Power Cycles^{*}

Francesco Casella^{*} Giovanni Mangola^{*} Dario Alfani^{**}

^{*} *Dipartimento di Elettronica, Informazione e Bioingegneria,
Politecnico di Milano, Milano, Italy*

(e-mail: francesco.casella@polimi.it, giovanni.mangola@polimi.it)

^{**} *Dipartimento di Energia, Politecnico di Milano, Italy
(e-mail: dario.alfani@polimi.it)*

Abstract: In this paper, the problem of controlling the thermodynamic state at the outlet of the air cooling unit in a supercritical CO₂ Brayton cycle is addressed. First-principle modelling analysis of the cooler model with boundary conditions representing the interaction with the full plant reveals that the dynamic response of the CO₂ outlet density to small changes of the cooling air flow has a much higher gain and a much more regular behaviour across the whole operating range of the system than the outlet temperature, suggesting to use the former variable for feedback control instead of the latter. Furthermore, it is shown how adaptive density feedback controllers can be designed with simple gain scheduling policies based on the plant load level and on the cooling air temperature.

Keywords: Modeling and simulation of power systems, Control system design, Control of renewable energy sources, Supercritical CO₂ Brayton cycles.

1. INTRODUCTION

Supercritical carbon dioxide (sCO₂) cycles for power generation are likely to play a relevant role in the future energy scenario and, over the past decade, have received increasing attention from industry, research institutions, and academia, as demonstrated by the large amount of research effort and investments. Thanks to the potential higher efficiency, to the simpler plant arrangement and to the faster transients allowed by the more compact turbine, sCO₂ Brayton cycles are commonly identified as the most promising technology to replace conventional steam Rankine cycles in a number of applications as concentrating solar power (CSP) (Binotti et al., 2017), nuclear (Dostal et al., 2004), coal (Alfani et al., 2019a), natural gas and waste heat recovery (WHR) (Astolfi et al., 2018). Note that, although the technology is deemed promising, there are no existing full-scale working prototypes of such plants at the moment. Experimental studies so far only involved lab-scale units, while full-scale plant studies, including the present one, are limited to design and simulation activities.

The critical point of carbon dioxide is near ambient temperature, about 31°C, and at about 74 bar pressure. sCO₂ power cycles take advantage of this property by compressing the carbon dioxide in a region close to the critical point, where the density is much larger than in standard ideal-gas Brayton cycles because of the remarkably low compressibility factor $Z = 0.2 \div 0.3$, resulting in much reduced compression work, hence much lower compressor power compared to the turbine power (Angelino, 1969).

Steady-state analysis and design of sCO₂ Brayton cycles always assumes that the main compressor operates with fixed pressure and temperature conditions over the entire operating range of the system, see e.g. Deshmukh et al. (2019), Tang et al. (2019), Moisseytsev et al. (2009), Moisseytsev and Sienicki (2011). However, small changes in temperature close to the critical point during plant operation can lead to large changes in the fluid density, significantly affecting the compressor operation and potentially reducing the cycle efficiency.

A robust and fast control system is thus required to keep compressor inlet conditions (corresponding to the cooler outlet conditions in the sCO₂ cycle) constant during load change ramps (Deshmukh et al., 2019). The approach taken in the literature is to control those conditions by means of a temperature feedback loop, see, e.g., (Liese et al., 2019). A notable exception is the paper by Hacks et al. (2019), who argue that the compressor inlet conditions in the slightly supercritical region are better characterized by measuring the density than by measuring the temperature, based on the thermodynamic properties of sCO₂ close to the critical point. This paper actually follows that suggestion, carrying out a model-based control design analysis with reference to an exemplary power sCO₂ cycle.

The large range of possible applications and the possible scarcity of water, coupled to the EU goal to reduce water consumption, makes the use of direct air-cooled Heat Rejection Units (HRUs) of great interest for sCO₂ systems. Therefore, an air cooler is considered as HRU in this paper. On the other hand, the higher variability of ambient air temperature compared to river, lake, or sea water temperature leads to possible issues in the control of the

^{*} This research work is supported by the European Commission under Horizon 2020 Grant 764690 - Project sCO2-Flex

operating conditions at compressor inlet, which need to be addressed.

This paper thus focuses on the control of the air cooling unit of the sCO₂ power generation system studied in the Horizon 2020 EU project SCO2-Flex, described in (Alfani et al., 2019b). The goal of the controller is to maintain the thermodynamic conditions of the fluid at the HRU outlet as close as possible to the required conditions at the main compressor inlet, which are close to the critical point, by modulating the cooling air flow. The aim of the paper is not to come up with a specific controller design, but rather to analyse the process dynamics by means of a first-principle dynamic model of the process and, based on that, draw some general conclusions on the control strategy. The main conclusion is that the cooler outlet *density* should be measured and used for feedback control, rather than the *temperature*.

The paper is organized as follows: in Section 2, a first-principles dynamic model of the process is presented; in Section 3, possible control structures are presented, trying to exploit the specific properties of the process; in Section 4, the results of the analysis are shown, motivating the use of density feedback for the process control. Section 5 concludes the paper with indications for future work.

2. PROCESS MODEL

The present study is motivated by the objective of the Horizon 2020 sCO₂-Flex project, which is the full design of a flexible 25 MW_{el} sCO₂ cycle, powered by a coal-fired boiler, or possibly by other sources such as solar power. The process flow diagram is shown in Fig. 1. This paper is focused on the control of the conditions at the HRU outlet (Fig. 1, bottom left). In order to keep the analysis as simple as possible, as done e.g. in (Liese et al., 2019), only the HRU is modelled in detail, while the rest of the plant is replaced by boundary conditions depending on the full plant load, which were previously computed in Alfani et al. (2019b).

More specifically, the mass flow rate and temperature of CO₂ at the HRU inlet (point 1 in Fig. 1) and the pressure at the HRU outlet (point 2 in Fig. 1) are assumed to have prescribed values, which depend on the load level and are the result of an optimization of the overall plant efficiency for each operating condition, obtained through a numerical code for the sCO₂-Flex plant steady-state simulation. Different values of the cooling air temperature will also be considered, but as the ambient air temperature changes slowly, the dynamic response to their changes is not of particular interest here.

The main assumption of this study is that the dynamic response of the thermodynamic conditions at the HRU outlet to changes of the cooling air flow rate is sufficiently decoupled from the other dynamic phenomena taking place in the rest of the plant. This implies that the indications drawn from the analysis carried out in this paper, where the HRU boundary conditions are considered to be fixed at each load level, can also be useful in the context of the plant-wide sCO₂ plant control.

The HRU model is a full nonlinear, first-principles model built in Modelica (Mattsson et al., 1998) using the Ther-

moPower library (Casella and Leva, 2005, 2006) and the ExternalMedia library (Casella and Richter, 2008) for access to sCO₂ fluid properties.

The object diagram of the model, taken from the full sCO₂-Flex plant model, is shown in Fig. 2: the component at the top describes the mass, momentum, and energy equations of a 1D, finite-volume model of the CO₂ flow, and the computation of the heat transfer to the tube walls using the well-known Gnielinski correlation. This component exchanges heat through a distributed 1D thermal port with a 1D thermal model of the tube walls, which in turn exchanges heat with a 1D model of the cooling air flow, through a component describing an ideal counter-current heat transfer configuration. The heat transfer coefficient between the cooling air flow and the external wall surface is assumed to be proportional to the mass flow rate to the power of 0.6.

All the 1D models are discretized with 30 finite volumes; note that a quite high number of volumes is necessary to describe the drastic changes of fluid properties along the tube length, in particular the specific heat capacity c_p towards the end of the CO₂ tube, where the thermodynamic conditions get closer to the critical point.

The HRU model, a component that will be later used for the modelling of the entire sCO₂ cycle plant of Fig. 1, is then completed by the simplified boundary components, as discussed previously in this Section. The model is used to compute the linearised dynamic responses to changes of the manipulated variable (the cooling air flow) around different equilibrium conditions corresponding to different values of the load of the full sCO₂-Flex plant, and to different values of the cooling air temperature. To this purpose, the values of the inlet mass flow rate and outlet pressure of the HRU are fixed to the steady-

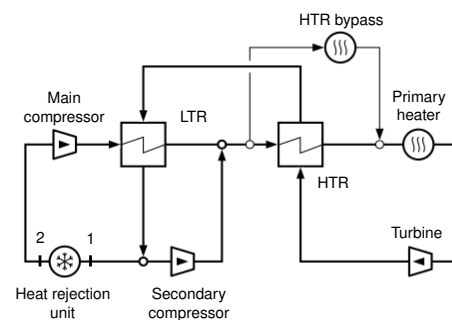


Fig. 1. Process flow diagram of the sCO₂-flex plant

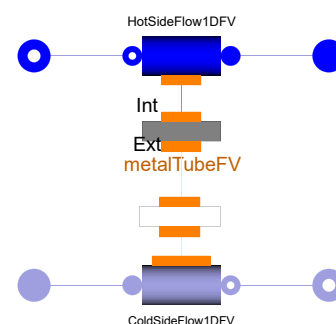


Fig. 2. Modelica diagram of the HRU model

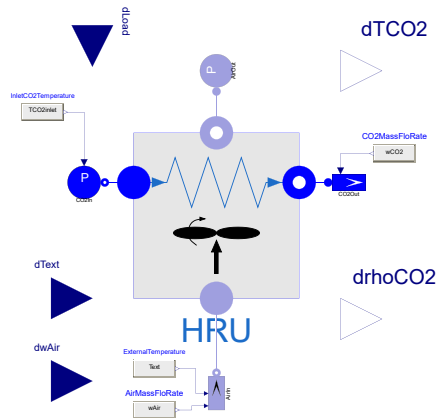


Fig. 3. Modelica diagram of the HRU fitted with boundary conditions

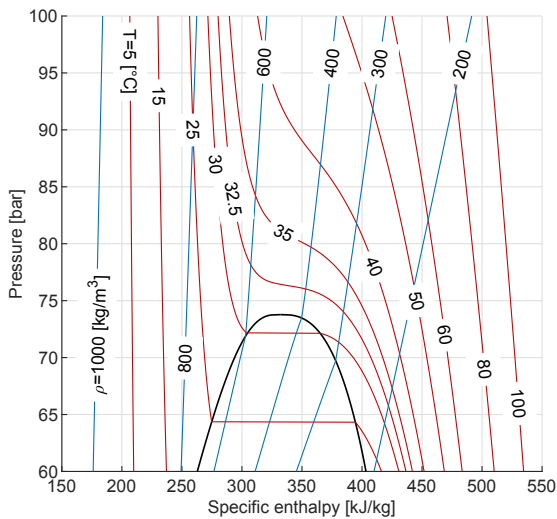


Fig. 4. p-h diagram of the CO₂, obtained through RefProp 9.1 (Lemmon et al., 2018)

state values corresponding to the specific plant load under consideration, while the static offset value of the air flow rate is computed using the HRU model to obtain the required steady-state HRU outlet density and temperature conditions, also considering different values of the cooling air temperature.

The Dymola tool was then used to process the Modelica model, to compute the steady-state solutions and to compute the linearized models around those steady-state solutions, the linearized model input being the small deviation of the cooling air flow rate around its offset value.

A final crucial consideration concerns the thermodynamic state at the HRU outlet. As already mentioned in Section 1, the sCO₂ cycle is designed on purpose with the thermodynamic conditions at the main compressor inlet (corresponding to the HRU outlet) close to the critical point, in order to exploit the real gas effect to obtain a high flow density and a corresponding low compression work. However, the thermodynamic behaviour of the fluid in that region is rather peculiar.

When removing thermal power from a fluid in a heat exchanger, the specific enthalpy h is reduced. Looking at the p-h diagram of Fig 4, in the regions to the left and to the right of the saturation dome, that correspond to liquid and superheated vapour or gas, the isothermal curves (in red) are almost vertical, meaning that changes of enthalpy basically correspond to changes of temperature. However, in the region where the HRU outlet operates, which is immediately above the critical point, those curves become almost horizontal instead, meaning that a change of enthalpy does not really correspond to a change in temperature. Moreover, the slope of those curves changes dramatically in the neighbourhood of the critical point, suggesting highly nonlinear behaviour of the temperature in that operating region.

If one looks at the isochoric lines (in blue) instead, corresponding to points with the same density, the behaviour in the HRU outlet operating region, slightly above the critical point, turns out to be very regular, with almost vertical lines. This means that in the neighbourhood of the critical point, the fluid density is a much more reliable and much more linear indicator of the enthalpy content of the fluid than the fluid temperature is.

This observation suggests the use of density instead of temperature as a better choice of controlled process variable for feedback control of the HRU outlet state.

3. PROCESS CONTROL STRUCTURES

In the context of the simplified process structure described in the previous section, four simple controller structures can be considered. The simplest possible ones are feedback control of HRU outlet temperature and feedback control of HRU outlet density, as shown in Fig 5.a-b. In the second case, the density must be measured directly, using sensors based on the Coriolis effect (Morris and Langari, 2016). In all cases, the cooling air mass flow rate, which is roughly proportional to the cooling fan speed, is used as the manipulated variable of the process.

Considering that the original sCO₂ power cycle which motivates this study is designed to work in the 20%–100% load range, one can expect a significant variation of the dynamic response of the process seen by the controller between the full-load case and the minimum-load case. One could then think of compensating this variation by introducing a simple form of gain scheduling, e.g., multiplying the controller output by the load level in p.u., as shown in Fig. 5.c-d.

It is then possible to assess which of the four proposed controller structures is the most effective one by evaluating the frequency response between small variations of the output u of the controller block C (before the multiplication node in the last two cases) and the corresponding variations of the process output T_{out} or ρ_{out} .

4. RESULTS OF THE ANALYSIS

The analysis proposed in Section 3 was carried out on the process model presented in Section 2. The Modelica tool Dymola was used to compute the steady-state operating conditions of the HRU corresponding to different load

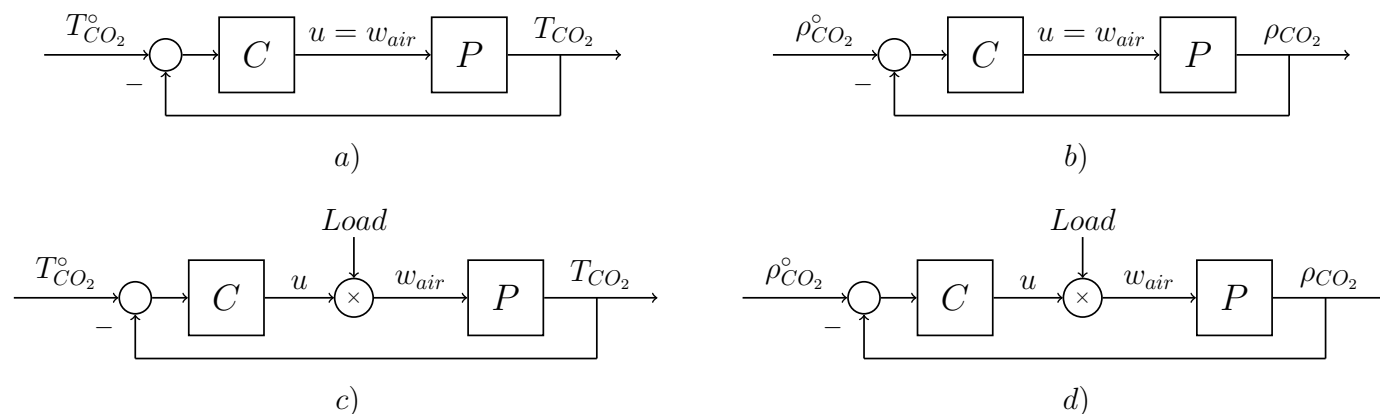


Fig. 5. Alternative process control structures

levels of the original sCO₂ power cycle, considering the design value of the cooling air, 20 °C. Then, the tool was used to compute linearized models at those equilibrium conditions, from which the frequency response of the transfer functions between the small changes of the cooling air mass flow rate and the temperature and density at the HRU outlet were obtained.

The obtained frequency responses, which correspond to the dynamic behaviour seen by the controller C in Fig. 5.a-b, turn out to be heavily affected by the load level, with changes of the static gain up to a factor five; hence, they are not particularly favourable for the design of the controller C, and thus not reported here due to space limitations.

The frequency responses of the transfer functions multiplied by the load level, which correspond to the dynamic behaviour seen by the feedback controller C in Fig. 5.c-d, are instead shown in Fig. 6. All variables have been normalized: the cooling air flow and the outlet fluid density are divided by their design value, while the outlet temperature is divided by the difference between HRU inlet and outlet temperature in design conditions.

The first important outcome is that the gain of the normalized transfer function is one order of magnitude higher in the case of the density feedback than in the case of the temperature feedback. This means that temperature controllers need to have much higher gains than density controllers, leading to much higher sensitivity to sensor noise.

For example, looking at the static gains of the transfer functions, a variation of 1% of the air flow rate corresponds to a change of 3.6 kg/m³ in the HRU outlet density, which is about 0.4% of the measurement range 0–1000 kg/m³ of the corresponding sensor, while it corresponds to a change of a meager 0.07 K of the outlet temperature, which is only 0.07% of the range of a temperature sensor calibrated in the range 0–100°C. It is then apparent how temperature feedback controllers will be a lot more critical from the point of view of sensor signal/noise ratio and of sensitivity to sensor noise than density feedback controllers.

Additionally, the temperature measurement may also be affected by significant additional phase lag due to the

temperature sensor inertia, which is not the case for the much faster density sensor.

The second important result is that the dynamic behaviour of the density response, once corrected by the load level, is only marginally affected by the load level itself, as is apparent from the fact that the Bode plots computed at different load levels are very close to each other. Conversely, despite the load correction, the gain of the transfer function to the temperature decreases by a factor five when the load is reduced from 100% to 45%, and then increases again by a factor three when the load is further reduced to 20%.

This means that a fixed-parameter density controller C used in the structure of Fig. 5.d can be designed to obtain good performance over the entire operating range of the plant, while some kind of much more involved adaptive or gain-scheduling controller C would be required for the temperature feedback structure of Fig. 5.c.

Notice how these conclusions can be drawn from the analysis of the process dynamics, regardless of the actual design and implementation of the controller C.

To complete the analysis, the effect of changes in the steady-state value of the cooling air temperature was analyzed. A reduction of the air temperature from the design value of 20 °C down to -5°C dramatically changes the gain of the transfer function seen by block C in Fig. 3.d. This can be easily explained, since a larger temperature difference between the cooling air and the CO₂ means that the same increase in air flow carries away more heat, thus increasing the transfer function gain.

However, if another multiplicative compensation by the factor $1/\Delta T$ is added at the controller output, where ΔT is the difference between the HRU outlet desired temperature and the cooling air temperature (see Fig. 7), the resulting transfer functions seen by the C controller have the frequency responses shown in Fig. 8, which are fairly insensitive to changes in both load level and external air temperature, except for the cases of low load and low external temperature.

Based on this result, if the control architecture of Fig. 7 is used, a fixed-parameter C controller is easily designed to cope with loads between 100% and about 50% and air temperatures between 20 °C and about 5°C. Handling the more extreme conditions may require either some more

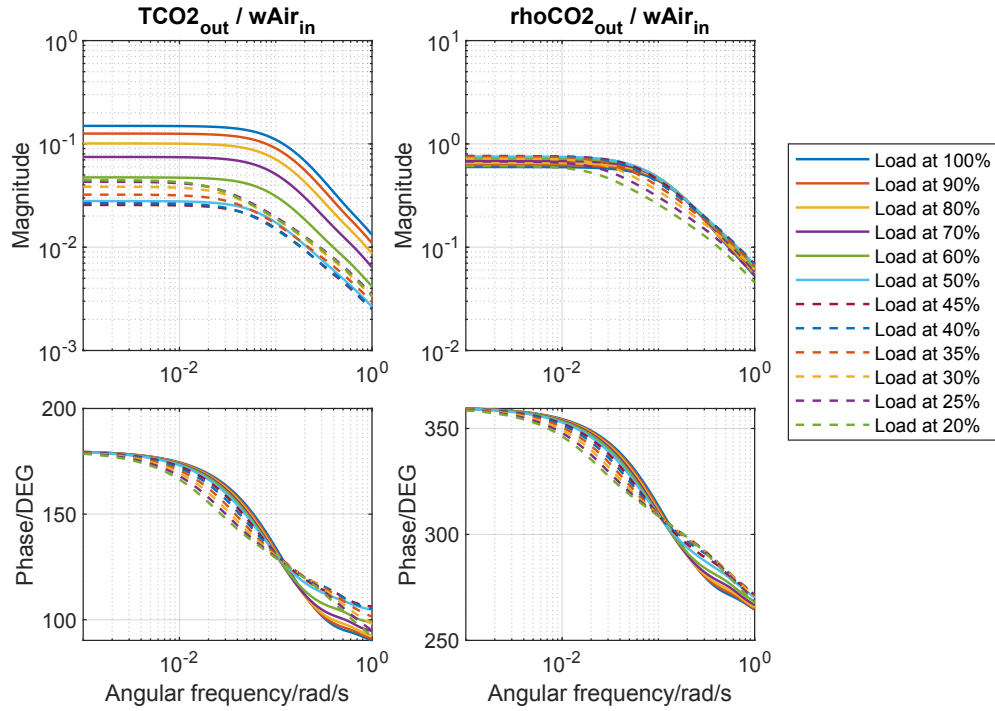


Fig. 6. Frequency responses of the process as seen by blocks C in Fig. 5.c-d – normalized units

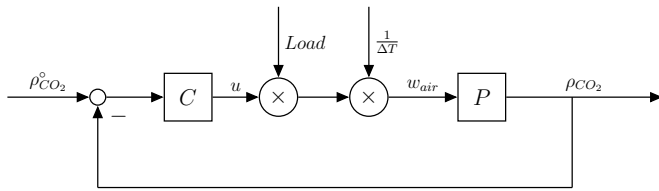


Fig. 7. Density feedback control with load and ΔT gain scheduling

sophisticated gain scheduling policy, or the use of a robust controller for the C block, that can manage the reduced magnitude and added phase lag in those conditions. Note that the reduction of the frequency response magnitude at low load and external temperature when using a fixed-parameter C block causes a reduction of the crossover frequency that will recover some of the lost phase margin, at the cost of a reduced controller bandwidth, which may be acceptable when operating close to the minimum load of the plant.

Last, but not least, note that the gain scheduling signals in Fig. 7 depend on exogenous disturbances (external air temperature) and set points (load, desired HRU outlet temperature), so that there are no stability issues due to parasite nonlinear feedback loops enabled by the gain-scheduling policy.

Summing up, compared to the conventional choice of temperature feedback, the use of HRU outlet density as a feedback variable provides higher process gain and signal-to-noise ratio, and makes it simpler to manage the variability of the small-signal dynamic response of the process due to the nonlinear effects of load and external

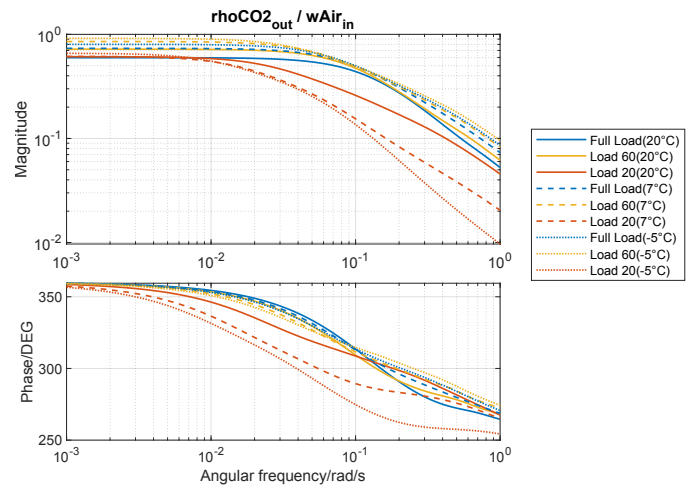


Fig. 8. Frequency response of the process as seen by block C in Fig. 7 – normalized units

temperature variations. It is expected that this will also be the case when considering plant-wide control of the full sCO_2 cycle of Fig. 1.

5. CONCLUSIONS AND FUTURE WORK

In this paper, the process dynamics of the air-cooled HRU in a sCO_2 power cycle was analyzed by means of a nonlinear first-principle model of the HRU, neglecting the dynamic interaction with the rest of the plant, which is described by representative boundary conditions, while still taking into account the operating conditions of the full plant in the range 20% – 100% of the design load.

The analysis of the process dynamics, which is also motivated by the thermodynamic behaviour of sCO₂ close to the critical point, suggests that the thermodynamic state of the fluid at the HRU outlet is more effectively and more easily controlled if the HRU outlet density is used for feedback, instead of the HRU outlet temperature; the density can be measured directly with Coriolis-force based sensors. Furthermore, the addition of a simple gain scheduling policies, based on the load level and on the difference between the desired CO₂ outlet temperature and the cooling air temperature, dramatically reduces the variability of the process seen by the feedback controller, facilitating the design of simple gain-scheduling controllers.

These ideas will be used when tackling the plant-wide control problem of the full sCO₂ power cycle, which is currently under evaluation, and are expected to provide useful indications also in that more general case.

The authors also believe that density-based control will also be more effective than temperature-based control in case a water-cooled HRU is used, since the nonlinear behaviour of sCO₂ is not really affected by the type of fluid used on the cold side of the heat exchanger, while the influence of the cooling medium temperature will be less important, since the variability of cooling water supply temperatures is much lower than that of ambient air.

REFERENCES

- Alfani, D., Astolfi, M., Binotti, M., Campanari, S., Casella, F., and Silva, P. (2019a). Multi Objective Optimization of Flexible Supercritical CO₂ Coal-Fired Power Plants. In *Proceedings ASME Turbo Expo: Power for Land, Sea, and Air*. doi:10.1115/GT2019-91789. V003T06A027.
- Alfani, D., Astolfi, M., Binotti, M., Macchi, E., and Silva, P. (2019b). Part-Load Operation Of Coal Fired sCO₂ Power Plants. In *3rd European supercritical CO₂ Conference September 19-20, 2019, Paris, France*, 1–9. doi:10.17185/dupublico/48897.
- Angelino, G. (1969). Real gas effects in carbon dioxide cycles. Technical report. doi:10.1115/69-GT-102.
- Astolfi, M., Alfani, D., Lasala, S., and Macchi, E. (2018). Comparison between ORC and CO₂ power systems for the exploitation of low-medium temperature heat sources. *Energy*, 161, 1250–1261. doi:10.1016/J.ENERGY.2018.07.099.
- Binotti, M., Astolfi, M., Campanari, S., Manzolini, G., and Silva, P. (2017). Preliminary assessment of sCO₂ cycles for power generation in CSP solar tower plants. *Applied Energy*, 204, 1007–1017. doi:10.1016/j.apenergy.2017.05.121.
- Casella, F. and Leva, A. (2005). Object-oriented modelling & simulation of power plants with modelica. In *Proceedings 44th IEEE Conference on Decision and Control and European Control Conference 2005*, 7597–7602. IEEE, EUCA, Seville, Spain.
- Casella, F. and Leva, A. (2006). Modelling of thermo-hydraulic power generation processes using Modelica. *Mathematical and Computer Modeling of Dynamical Systems*, 12(1), 19–33. doi:10.1080/13873950500071082.
- Casella, F. and Richter, C.C. (2008). ExternalMedia: a library for easy re-use of external fluid property code in Modelica. In B. Bachmann (ed.), *Proceedings 6th International Modelica Conference*, 157–161. Modelica Association, Bielefeld, Germany. URL <http://www.modelica.org/events/modelica2008/Proceedings/sessions/session2b1.pdf>.
- Deshmukh, A., Kapat, J., and Khadse, A. (2019). Transient Thermodynamic Modeling of Air Cooler in Supercritical CO₂ Brayton Cycle for Solar Molten Salt Application. In *Proceedings ASME Turbo Expo: Power for Land, Sea, and Air*. doi:10.1115/GT2019-91409. V009T38A023.
- Dostal, V., Driscoll, M., and Hejzlar, P. (2004). A Supercritical Carbon Dioxide Cycle for Next Generation Nuclear Reactors. *Technical Report MIT-ANP-TR-100*, 1–317.
- Hacks, A.J., Schuster, S., and Brillert, D. (2019). Stabilizing effects of supercritical CO₂ fluid properties on compressor operation. *Int. J. of Turbomachinery Propulsion and Power*, 4(20). doi:10.3390/ijtpp4030020.
- Lemmon, E.W., , Bell, I.H., Huber, M.L., and McLinden, M.O. (2018). NIST Standard Reference Database 23: Reference Fluid Thermodynamic and Transport Properties-REFPROP, Version 9.1, National Institute of Standards and Technology. doi:10.18434/T4JS3C.
- Liese, E., Mahapatra, P., and Jiang, Y. (2019). Modeling and Control of a Supercritical CO₂ Water Cooler in an Indirect-Fired 10MWe Recompression Brayton Cycle Near Critical Conditions. In *Proceedings ASME Turbo Expo: Power for Land, Sea, and Air*. doi:10.1115/GT2019-90496. V009T38A009.
- Mattsson, S.E., Elmquist, H., and Otter, M. (1998). Physical system modeling with Modelica. *Control Engineering Practice*, 6(4), 501–510.
- Moisseytsev, A., Kulesza, K.P., Sienicki, J.J., Division, N.E., and Univ., O.S. (2009). Control system options and strategies for supercritical CO₂ cycles. doi:10.2172/958037.
- Moisseytsev, A. and Sienicki, J.J. (2011). Development of the ANL plant dynamics code and control strategies for the supercritical carbon dioxide brayton cycle and code validation with data from the Sandia small-scale supercritical carbon dioxide brayton cycle test loop. Technical report. doi:10.2172/1040687.
- Morris, A.S. and Langari, R. (2016). Chapter 16 - flow measurement. In A.S. Morris and R. Langari (eds.), *Measurement and Instrumentation (Second Edition)*, 493 – 529. Academic Press, Boston, second edition edition. doi:10.1016/B978-0-12-800884-3.00016-2.
- Tang, C.J., McClung, A., Hofer, D., and Huang, M. (2019). Transient Modeling of 10 MW Supercritical CO₂ Brayton Power Cycles Using Numerical Propulsion System Simulation (NPSS). In *Proceedings ASME Turbo Expo: Power for Land, Sea, and Air*. doi:10.1115/GT2019-91443. V009T38A024.